Clinical efficacy of haematopoietic stem cell transplantation for adult adrenoleukodystrophy

Takashi Matsukawa, Tomotaka Yamamoto, Akira Honda, Takashi Toya, Hiroyuki Ishiura, Jun Mitsui, Masaki Tanaka, Akihito Hao, Akihito Shinohara, Mizuki Ogura, Keisuke Kataoka, Sachiko Seo, Keiki Kumano, Masataka Hosoi, Kensuke Narukawa, Megumi Yasunaga, Hiroaki Maki, Motoshi Ichikawa, Yasuhito Nannya, Yoichi Imai, Tsuyoshi Takahashi, Yuji Takahashi, Yuki Nagasako, Kyoko Yasaka, Kagari Koshi Mano, Miho Kawabe Matsukawa, Toji Miyagawa, Masashi Hamada, Kaori Sakuishi, Toshihiro Hayashi, Atsushi Iwata, Yasuo Terao, Jun Shimizu, Jun Goto, Harushi Mori, Akira Kunimatsu, Shigeki Aoki, Shin Hayashi, Fumihiko Nakamura, Syunya Arai, Kazunari Momma, Katsuhisa Ogata, Toshikazu Yoshida, Osamu Abe, Johji Inazawa, Tatsushi Toda, Mineo Kurokawa, Shoji Tsuji

Supplementary Figure 1A. Changes in Barthel index

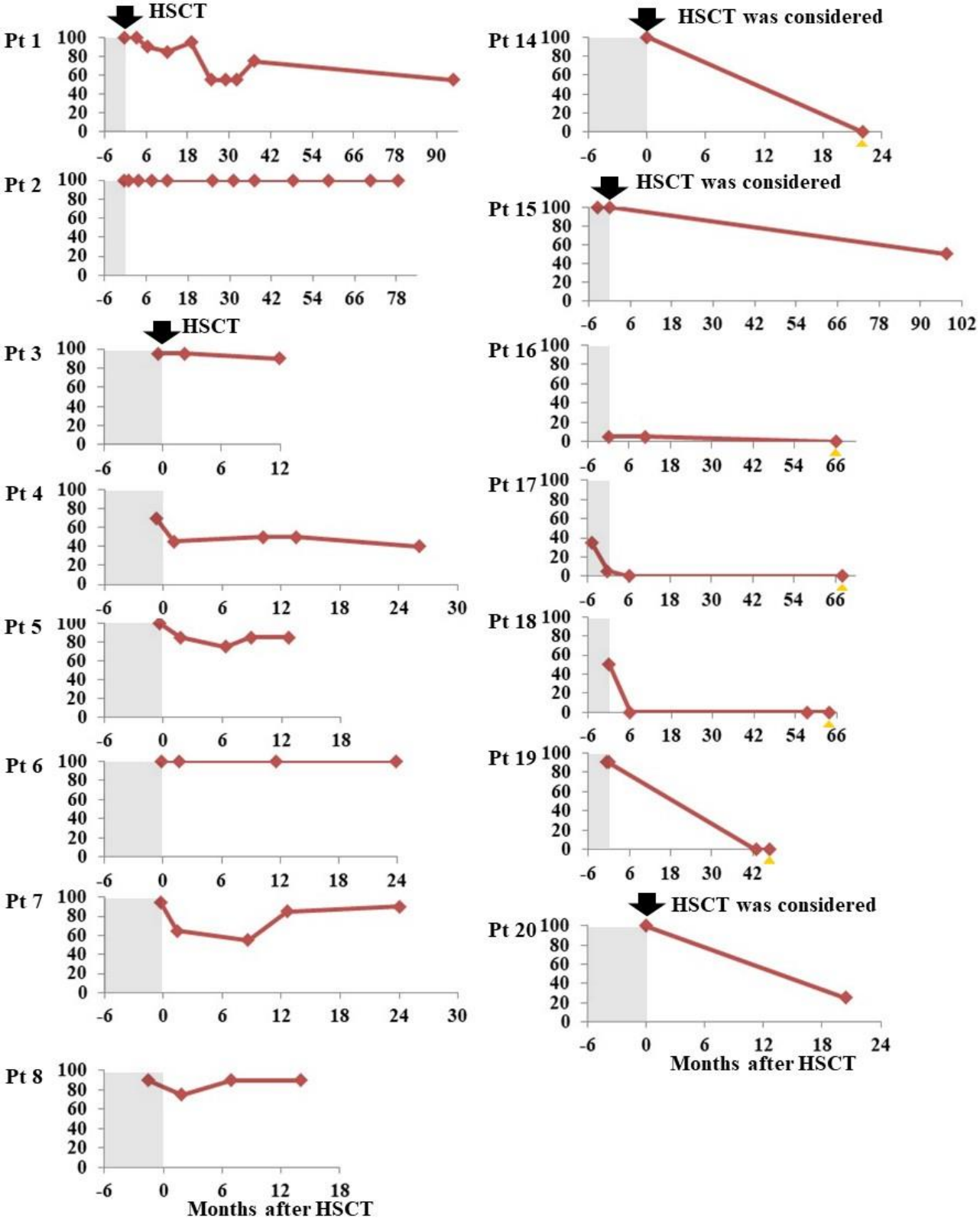

Barthel index assesses ADL of patients. We focused on patients whose rating scales (Barthel index, EDSS, and ALD-DRS) had been evaluated before HSCT and for a period longer than 11.9 months after HSCT. The horizontal axis in the left panel shows the months after HSCT and that in the right panel shows the months after considering HSCT. The vertical axis shows Barthel index scores. ‘100’ and ‘0’ are the best and worst scores, respectively. Yellow triangles indicate the death of patients. Pt, Patient.

Supplementary Figure 1B. Changes in EDSS

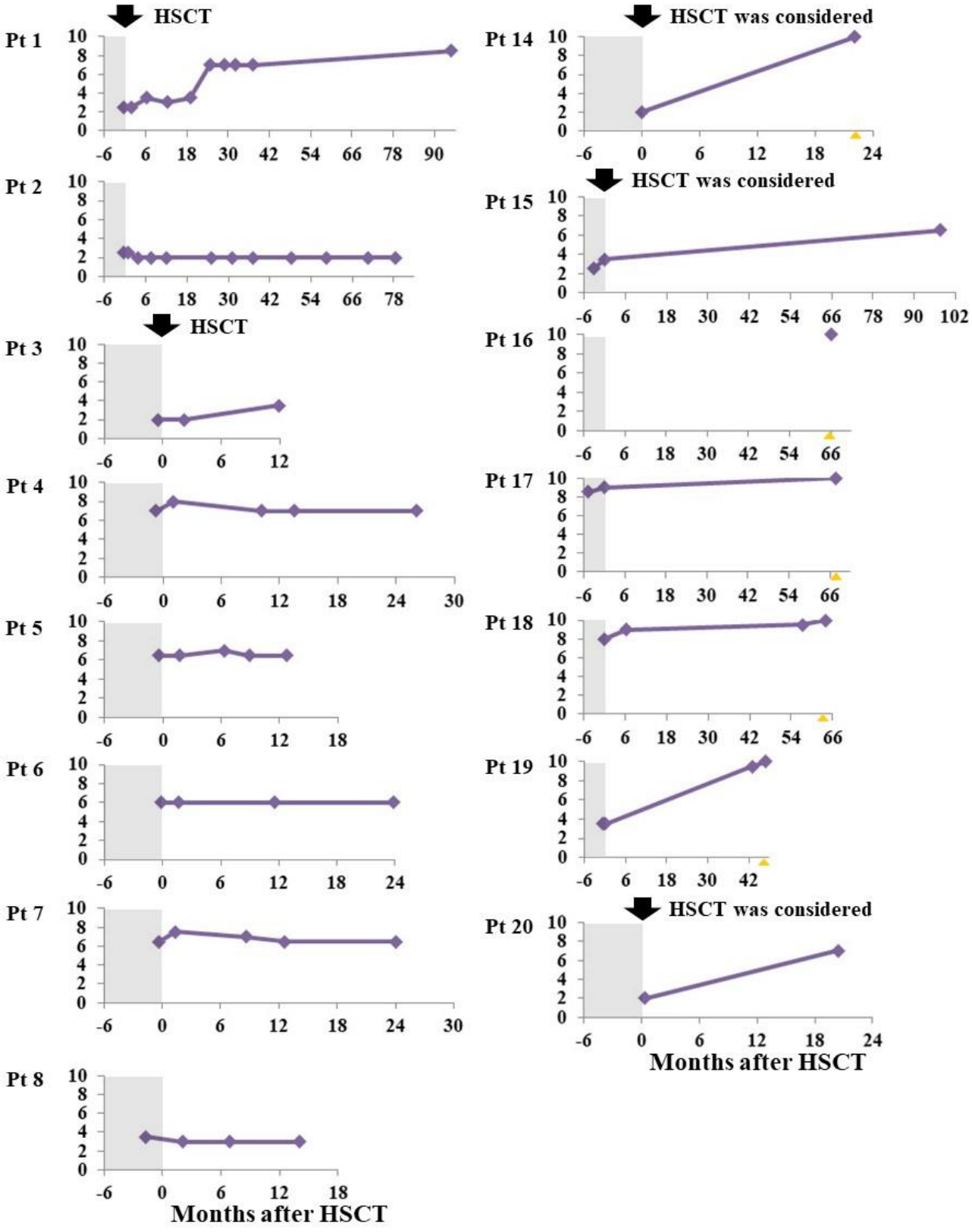

EDSS assesses the severity of the disability of the patients, mainly focusing on walking ability. We focused on patients whose rating scales (Barthel index, EDSS, and ALD-DRS) had been evaluated before HSCT and for a period longer than 11.9 months after HSCT. The horizontal axis in the left panel shows the months after HSCT and that in the right panel shows the months after considering HSCT. The vertical axis shows EDSS scores. '0' and '10' are the best and the worst scores, respectively. Yellow triangles indicate the death of patients. Pt, Patient.

Supplementary Figure 1C. Changes in ALD-DRS

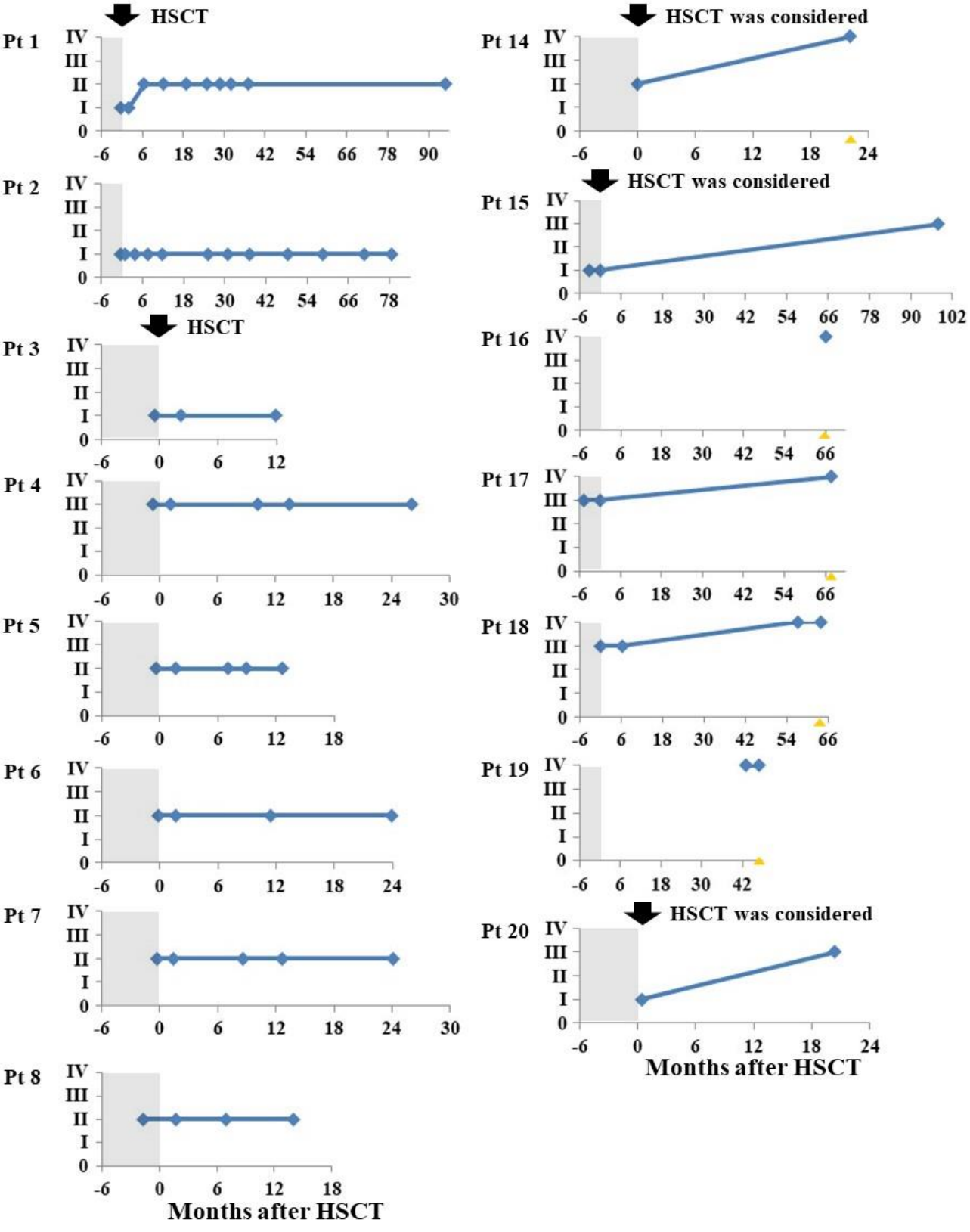

ALD-DRS assesses the level of the degree of disability of patients with cerebral form ALD, which was developed to specifically assess the functional disability of patients with CCALD. We focused on patients whose rating scales (Barthel index, EDSS, and ALD-DRS) had been evaluated before HSCT and for a period longer than 11.9 months after HSCT. The horizontal axis in the left panel shows the months after HSCT and that in the right panel shows the months after considering HSCT. The vertical axis shows ALD-DRS grade. ‘0’ and ‘IV’ are the best and worst grades, respectively. Yellow triangles indicate the death of patients. Pt, Patient.

Supplementary Figure 2. Changes in brain MRI findings before and after HSCT in Patients 1, 3, 5, 6, 8, and 9–12.

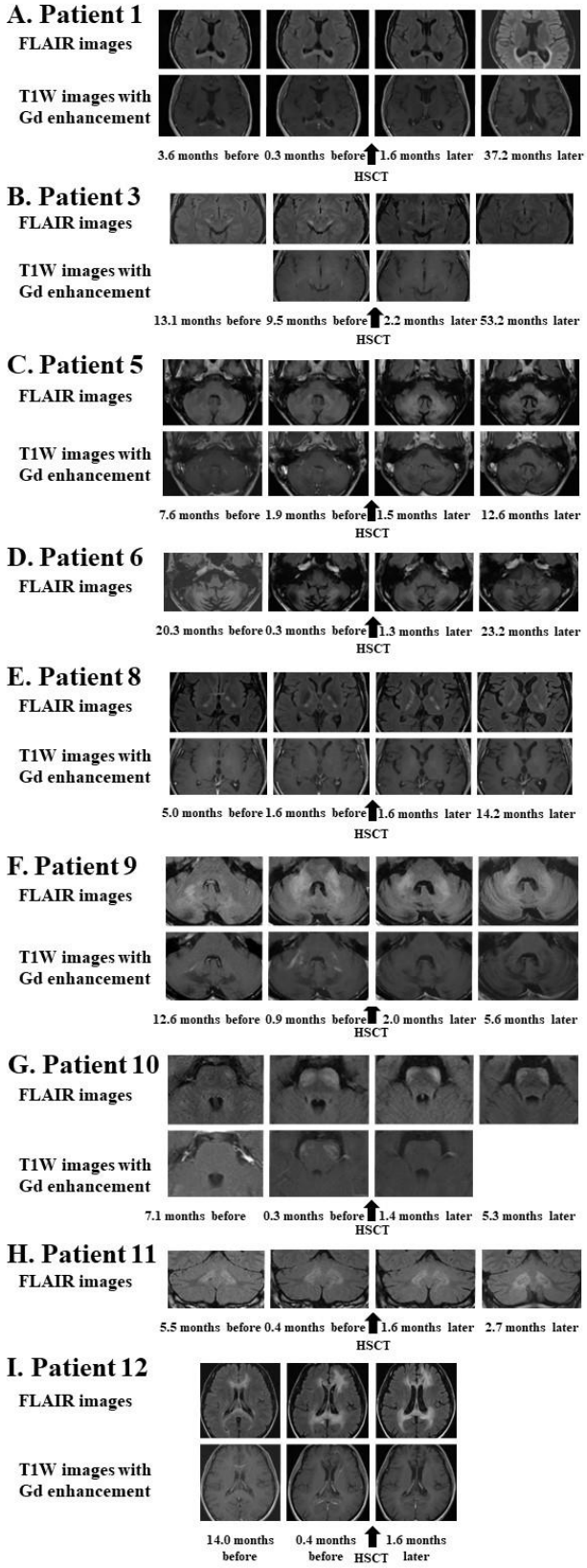

Panel A shows axial images of the splenium of the corpus callosum and around the lateral ventricles obtained by FLAIR imaging (upper panels) and T1W imaging with Gd enhancement (lower panels) on brain MRI before and after HSCT in Patient 1. The white matter lesion in the splenium of the corpus callosum was enhanced before HSCT but disappeared (lower panels) after HSCT. The white matter lesions in the splenium of the corpus callosum became small (upper panels) after HSCT.

Panel B shows axial FLAIR images (upper panels) and T1W images with Gd enhancement (lower panels) of the midbrain on brain MRI before and after HSCT in Patient 3. The white matter lesions in the brachia of the inferior colliculi were enhanced before HSCT but became obscure (lower panels) after HSCT. The white matter lesions in the pyramidal tracts in the brainstem and the brachia of the inferior colliculi became obscure (upper panels) after HSCT.

Panel C shows axial FLAIR images of the brainstem and cerebellum (upper panels) and T1W images with Gd enhancement (lower panels) before and after HSCT in Patient 5. The white matter lesions in the cerebellum were enhanced before HSCT but no longer enhanced (lower panels) after HSCT. The Gd enhancement was clearly shown by infusion of a double dose of the gadolinium contrast for MRI performed 7.6 months before HSCT. The white matter lesions in the cerebellum and brainstem enlarged until 1.5 months after HSCT, but the lesions did not enlarge (upper panels) subsequently. Mild cerebellar and brainstem atrophy slightly progressed.

Panel D shows axial FLAIR images of the brainstem and the cerebellum before and after HSCT in Patient 6. The white matter lesions in the cerebellum gradually enlarged before HSCT but did not enlarge after HSCT. Although a double dose of the gadolinium contrast was infused when we performed MRI 0.3 months before HSCT, no evident enhancement was detected in Patient 6.

Panel E shows axial FLAIR images of the internal capsules (upper panels) and T1W images with Gd enhancement (lower panels) on brain MRI before and after HSCT in Patient 8. The white matter lesions in the internal capsules were enhanced before HSCT but no longer enhanced (lower panels) after HSCT. The white matter lesions in the internal capsules enlarged before HSCT but did not enlarge (upper panels) after HSCT.

Panel F shows axial FLAIR images of the cerebellum, brainstem, and middle cerebellar peduncles (upper panels) and T1W images with Gd enhancement (lower panels) on brain MRI before and after HSCT in Patient 9. The white matter lesions in the cerebellum, brainstem, and middle cerebellar peduncles enlarged and were Gd-enhanced before HSCT. Gd-enhanced lesions disappeared (lower panels) after HSCT.

Panel G shows axial FLAIR images of the cerebellum and brainstem (upper panels) and

T1W images with Gd enhancement (lower panels) on brain MRI before and after HSCT in Patient 10. The white matter lesions in the pyramidal tracts and the auditory pathway enlarged and were Gd-enhanced before HSCT. The white matter lesion became small (upper panels) and Gd-enhanced lesions became obscure (lower panels) after HSCT.

Panel H shows coronal FLAIR images of the cerebellum before and after HSCT in Patient 11. The white matter lesions in the cerebellum gradually enlarged before HSCT but did not enlarge after HSCT. No evident enhancement was detected in Patient 11 before and after HSCT.

Panel I shows axial FLAIR images (upper panels) and T1W images with Gd enhancement (lower panels) of the genu and splenium of the corpus callosum, and around the lateral ventricles on brain MRI before and after HSCT in Patient 12. The white matter lesions in the frontal, parietal, occipital, and temporal lobes, and the genu and splenium of the corpus callosum enlarged before HSCT, but did not enlarge (upper panels) after HSCT. The white matter lesions in the left frontal lobe and the genu and splenium of the corpus callosum, and around the lateral ventricles were Gd-enhanced before HSCT, but the Gd-enhanced lesions became obscure (lower panels) after HSCT.

Supplementary Figure 3. Reduction in size of white matter lesions and atrophic changes of the brainstem and cerebellum in brain MRI in Patients 1, 4, and 5 after HSCT.

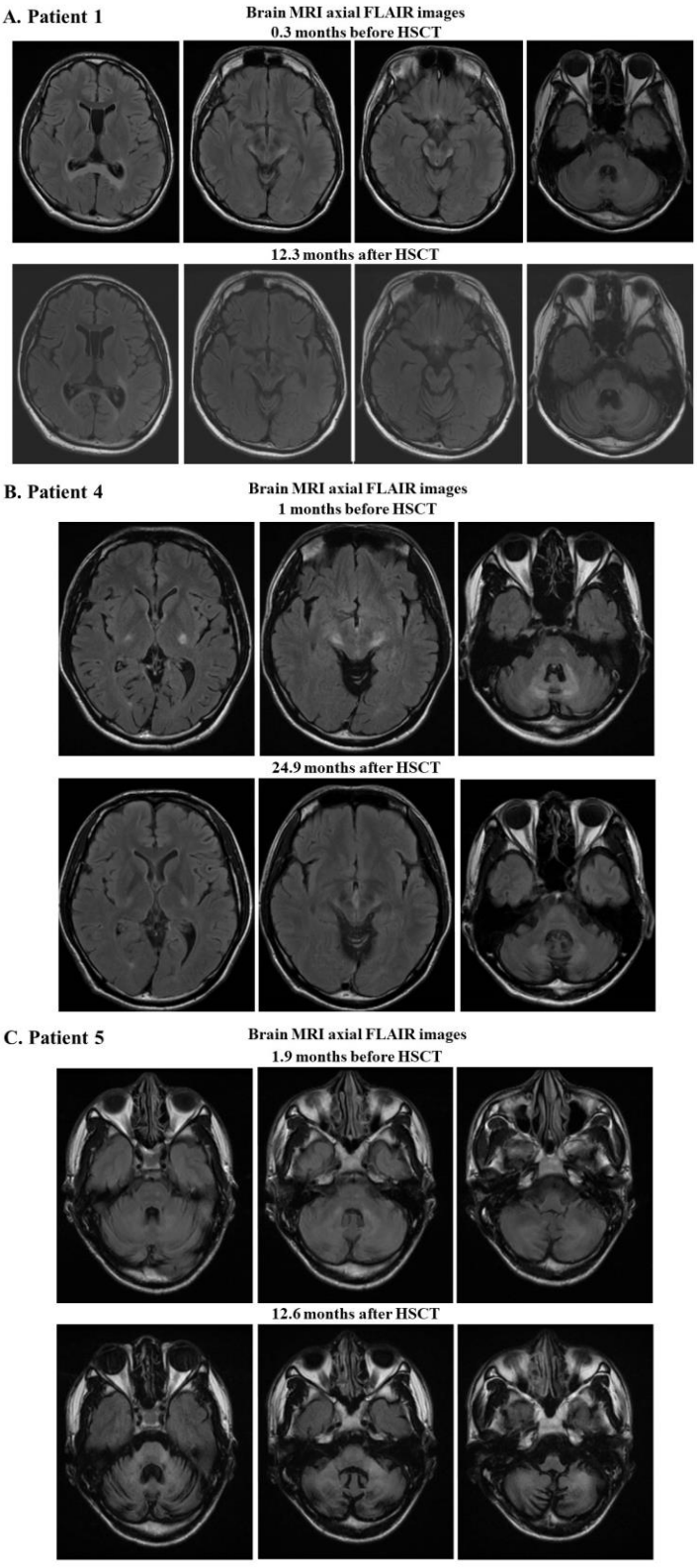

Panel A shows axial images of the brainstem, cerebellum, and around the lateral ventricles obtained by FLAIR imaging on brain MRI before and after HSCT in Patient 1. The white matter lesions in the auditory pathway became small even taking the mild atrophic change of the brainstem into consideration after HSCT. In addition, reduction of the lesions of the splenium of the corpus callosum is obvious after HSCT.

Panel B shows axial images of the brainstem and cerebellum and around the lateral ventricles obtained by FLAIR imaging on brain MRI before and after HSCT in Patient 4. The white matter lesions in the pyramidal tracts and cerebellum became small even taking the mild atrophic change of the brainstem and cerebellum into consideration after HSCT.

Panel C shows axial images of the brainstem and cerebellum obtained by FLAIR imaging on brain MRI before and after HSCT in Patient 5. The white matter lesions in the brainstem and cerebellum stabilized after HSCT. The atrophic changes of the brainstem and cerebellum progressed after HSCT.

Supplementary Figure 4. Changes in brain MRI findings in patients with AMN-Cer, ACALD, and cerebello-brainstem form ALD who did not undergo HSCT.

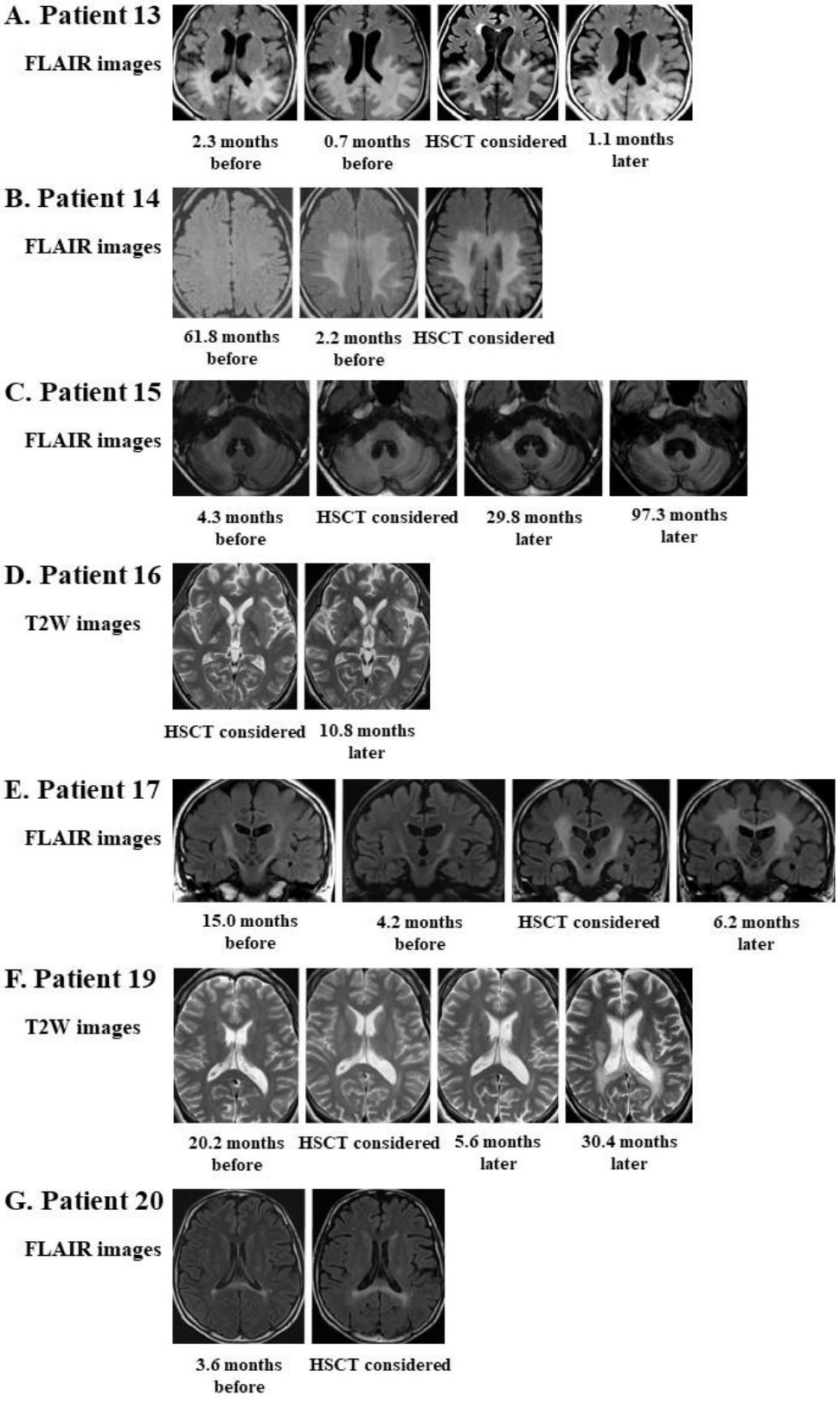

Panel A shows axial FLAIR images of the splenium of the corpus callosum and around the lateral ventricles on brain MRI before and after considering HSCT in Patient 13. Brain MRI showed diffuse white matter lesions involving the splenium of the corpus callosum and the occipital lobes.
Panel B shows axial FLAIR images of the parietal lobes on brain MRI before and after considering HSCT in Patient 14. Brain MRI showed diffuse white matter lesions involving the parietal lobes from 2.2 months before considering HSCT.
Panel C shows axial FLAIR images of the cerebellum, the middle cerebellar peduncles, and the brainstem on brain MRI before and after considering HSCT in Patient 15. Brain MRI showed white matter lesions in the cerebellum and the middle cerebellar peduncles, and progressive atrophy of the cerebellum, middle cerebellar peduncles, and brainstem.
Panel D shows axial T2-weighted (T2W) images around the lateral ventricles on brain MRI before and after considering HSCT in Patient 16. Brain MRI showed enlarged white matter lesions involving the pyramidal tracts in the internal capsules.
Panel E shows coronal FLAIR images around the lateral ventricles on brain MRI before and after considering HSCT in Patient 17. Brain MRI showed enlarged white matter lesions involving the pyramidal tracts in the internal capsules and the parietal lobes.
Panel F shows axial T2W images of the splenium of the corpus callosum and around the lateral ventricles on brain MRI before and after considering HSCT in Patient 19. Brain MRI showed enlarged white matter lesions involving the splenium of the corpus callosum, the occipital lobes, and the pyramidal tracts in the internal capsules.
Panel G shows axial FLAIR images of the splenium of the corpus callosum and around the lateral ventricles on brain MRI before and after considering HSCT in Patient 20. Brain MRI showed enlarged white matter lesions involving the splenium of the corpus callosum, the occipital lobes, and the pyramidal tracts in the internal capsules.

Supplementary Table 1. Primers for amplification of *ABCD1* for chimerism analysis using Miseq.

Primer name	Sequences	Primer length (bp)	Amplicon size (bp)
R518W_F_Patient1	5'- CCCTGCAGGTGGAGGAAGG	19	170
R518W_R_Patient1	5'- GCACGGGCTTCCTTACCTCTG	21	
Intron2_F_Patient2	5'- AGTTGAGTTGCGCAATGGAGTC	22	697
Xq28_R_Patient2	5'- GGGTAAGTATGACTAACCTGATACACAG	28	
Intron2_F_Patient2	5'- AGTTGAGTTGCGCAATGGAGTC	22	636
Chr13p11.2_R_Patient2	5'- ACAGCTACAGTACTGGGAGGAG	22	
H667N_F_Patient3	5'- GGGAGGAGGTGGCCTGGC	18	199
H667N_R_Patient3	5'- CAGCCGCTGCTTCTCCTCC	19	
E609K_F_Patient4	5'- GCCCCCGGGTCTGGGTG	17	204
E609K_R_Patient4	5'- CTCCCCACAGCTGCTACTTCC	21	
E609K _F_Patient5	5'- GCCCCCGGGTCTGGGTG	17	204
E609K _R_Patient5	5'- CTCCCCACAGCTGCTACTTCC	21	
R554H_F_Patient6	5'- CGTGTGAGCGTGGCATGTGG	20	228
R554H _R_Patient6	5'- ATGTGGTGCAGGTGCACGAC	20	
G277R_F_Patient7	5'- CGGCCTCGTGGTGTTCCTC	19	200
G277R _R_Patient7	5'- ACACGCTTCCCTCCGTGCC	19	
Q472Rfs_F_Patient8	5'- GCACGCAGACTCCCCAGAATG	21	209/207[*1]
Q472Rfs _R_Patient8	5'- ATATGTGCGTGGCTGGCGC	19	

[*1], The amplicon sizes derived from the wild-type allele and that derived from the mutant allele were 209 and 207 bp, respectively.

Supplementary Table 2. Primers and probes for chimerism analysis using droplet digital PCR.

Primer/Probe name	Sequences	Primer/Probe length (bp)
Y174S_F_Patient9_11	5'- CTGTCGTTCCGCAG	14
Y174S_R_Patient9_11	5'- CGGTAGTAGGTCTGCT	16
Y174S_mut_Probe_Patient9_11	5'- (FAM)-AGAAGGAGAGGCGGTAG	17
Y174S_wt_Probe_Patient9_11	5'- (HEX)-AGAAGTAGAGGCGGTAGG	18
Y174C_F_Patient10	5'- CTGTCGTTCCGCAG	14
Y174C_R_Patient10	5'- CGGTAGTAGGTCTGCT	16
Y174C_mut_Probe_Patient10	5'- (FAM)-AGAAGCAGAGGCGGT	15
Y174C_wt_Probe_Patient10	5'- (HEX)-AGAAGTAGAGGCGGTAGG	18

Supplementary Table 3. Results of chimerism analysis of bone marrow cells from donors and recipients after HSCT.

Results of microsatellite analysis for sex-matched HSCT

Patient 2

Months after HSCT	0.9	2.8
Percentage of DNAs from the recipient (%)	<10	<10

Patient 4

Months after HSCT	0.9
Percentage of DNAs from the recipient (%)	<10

Patient 5

Months after HSCT	0.9	5.9	13.0
Percentage of DNAs from the recipient (%)	<10	<10	<10

Patient 6

Months after HSCT	1.1	11.6
Percentage of DNAs from the recipient (%)	<10	<10

Patient 7

Months after HSCT	0.9	8.5	12.8
Percentage of DNAs from the recipient (%)	<10	<10	<10

Patient 9

Months after HSCT	1.0
Percentage of DNAs from the recipient (%)	<10

Patient 10

Months after HSCT	0.7
Percentage of DNAs from the recipient (%)	<10

Patient 11

Months after HSCT	1.1
Percentage of DNAs from the recipient (%)	<10

Results of fluorescence *in situ* hybridization analysis for sex-mismatched HSCT

Patient 1

Months after HSCT	1.1	3.2	13.3
Percentage of cells from the recipient (%)	1.5	0.5	0.5

Patient 3

Months after HSCT	1.0	1.9
Percentage of cells from the recipient (%)	3	1

Patient 8

Months after HSCT	0.9
Percentage of cells from the recipient (%)	0

Patient 12

Months after HSCT	1.0
Percentage of cells from the recipient (%)	0.5

The microsatellite analysis of bone marrow cells after HSCT in Patients 2, 4–7, and 9–11 showed that the percentages of the DNA from the recipient with respect to those from their donors were below measurable limits (<10%), and the fluorescence *in situ* hybridization analysis of bone marrow cells after HSCT in Patients 1, 3, 8, and 12

showed that the percentages of cells from the recipient with respect to those from their donors were equal to or less than 3%.